Submitted to

International Europhysics Conference on High Energy Physics, July 12, 2001, Budapest
EPS 2001: Abstract: **877**
Parallel Session **13**

www-h1.desy.de/h1/www/publications/conf/conf_list.html

Electron polarization measurement using a Fabry-Pérot cavity at HERA

E. Barrelet[1],V. Brisson[2], M. Jacquet-Lemire[2], A. Reboux[2],
C. Pascaud[2], Z. Zhang[2], F. Zomer[2]
and the POL2000 group[3]
[1]LPNHE Jussieu, IN2P3-CNRS
[2]Laboratoire de l'Accélérateur Linéaire, IN2P3-CNRS et Université de Paris-Sud
B.P. 34, F-91898 Orsay Cedex, France
[3]members from DESY, HERMES, H1 and ZEUS[1]

Abstract

A new Compton longitudinal polarimeter for HERA is under construction. The key component of the calorimeter is a Fabry-Pérot cavity located around the electron beam pipe. With such an optical cavity, a continuous laser power of 5 kW can be achieved leading to backscattered photon rate around one per bunch crossing. This 'few-photon mode' will allow a very precise determination of the calorimeter response with little systematic uncertainty. The electron polarization measurement at the per mill level is expected.

[1]See DESY PRC-99-01 for a detailed list of members of this group. Contact Ties.Behnke@desy.de

1 Introduction

The study of polarized electron-proton scattering at very high energies will be one of the major new physics topics after the upgrade of the HERA storage ring. The colliding-beam experiments H1 and ZEUS will for the first time have access to longitudinally polarized leptons. This will allow detailed studies of the helicity structure of the weak currents.

To fully exploit the potential of the machine and the luminosity to be delivered to the experiments, a significant upgrade of the existing longitudinal polarimeter (LPOL) has been proposed [1, 2]. The main components of the LPOL are a Fabry-Pérot cavity, a continuous wave laser of 0.7 W, a series of optical components to circularly polarize the laser light, a system of monitoring devices to measure and control the properties of the laser beam, a feedback system for control the frequency of the laser and to keep the cavity in resonance, and a fast data acquisition system to store all histograms needed for a polarization measurement on a bunch-by-bunch basis. The heart of the polarimeter is the high finesse monolithic Fabry-Pérot cavity, which allows to reach an effective power of the laser close to 5 kW, sufficient to obtain one backscattered photon per bunch crossing. With this system the statistical uncertainty of the polarization can be reduced to 0.1% per minute and per group of bunches in HERA, or 1% per minute and per bunch.

The structure of this paper is as follows. We will start in Sec.2 with a short description of the new LPOL and point out the difference with the existing ones. The necessities of having a fast and precise polarimeter is discussed in Sec.3, followed by a conclusion in Sec.4.

2 The New Longitudinal Polarimeter

At HERA, the electron or positron beam of 27.5 GeV in collision with the proton beam of 820-920 GeV is naturally polarized transversely through the emission of synchrotron radiation which is known as the Sokolov-Ternov effect [3]. Longitudinal polarization at East area near the HERMES experiment was achieved since 1994 by installing a pair of spin rotators. During the upgrade, the H1 and ZEUS interaction regions have also been equipped with spin rotators. Currently the measurement of the electron[2] polarization at HERA is done with two different devices. The transverse polarimeter (TPOL), which is installed in the West area of HERA, measures the polarization of the transversely polarized beam (Fig.1). The LPOL in contrast measures the longitudinal polarization of the beam near the HERMES interaction point. Since the absolute value of the degree of polarization of the electron beam is the same everywhere in the ring, the location of the polarization measurement is not confined to the experiment's interaction region.

The principle of the measurement relies on the non-destructive method of detecting backscattered photons produced in Compton scattering of an intense circularly polarized laser (photon) beam off the electron beam. The transverse polarization is measured from the vertical asymmetry, whereas the longitudinal polarization is determined from the energy asymmetry. The current statistical precision of the LPOL is around 1% for 2 minutes of data taking averaged

[2]Unless stated otherwise, the word "electron" will refer to both electron and positron in the following.

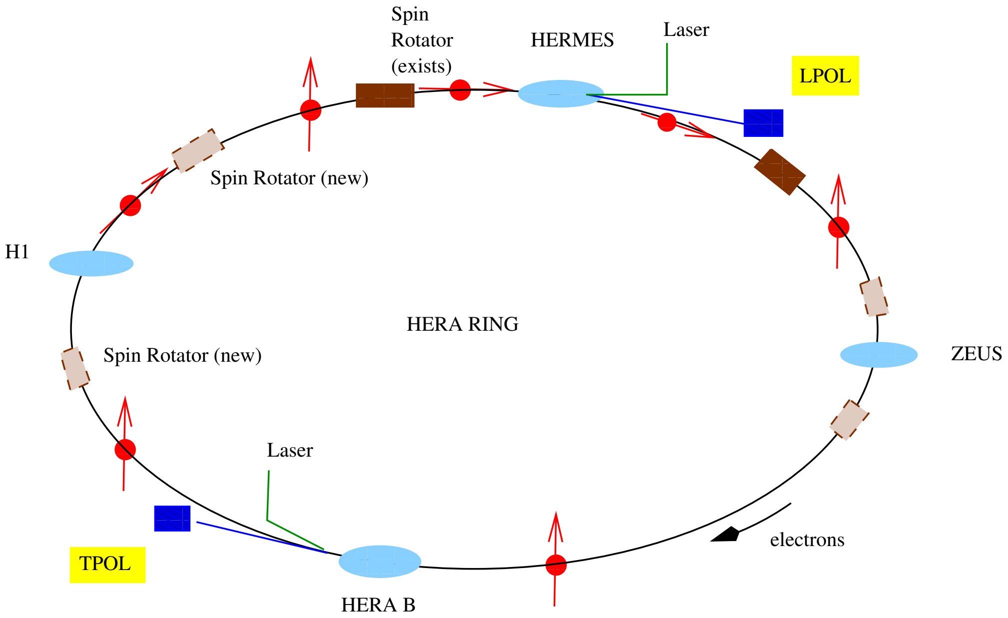

Figure 1: A schematic view of the HERA ep collider showing the locations of the interaction points, the spin rotators, and the longitudinal and transverse polarimeters (LPOL, TPOL).

over all bunches in the ring (up to 190). The systematic uncertainty is about 2% which is dominated by the energy scale uncertainty of the calorimeter measuring the backscattered photons in multi-photon mode[3]. To reach a same statistical precision for a single bunch, more than 30 minutes is required due to the low pulsed laser frequency (up to 100 Hz). The statistical precision of the TPOL is 1% per minute again averaged over all bunches (the current TPOL data acquisition (DAQ) system does not allow the differentiation of bunch to be made). The systematic uncertainty is about twice that of the LPOL due mostly to the limited statistics of the dedicated rise-time runs taken with a flat machine and needed to define the absolute polarization scale.

The new longitudinal polarimeter is under construction and will be installed next to the existing LPOL during the shutdown in the Spring of 2002. The new LPOL should provide the most precise measurement of the polarization with a statistical error of 0.1% (0.3%) for the colliding (non-colliding) bunches and 1% per minute for every single bunch, and a systematic error at per mill level.

[3]Three different modes of operation can be distinguished for a polarimeter detecting the backscattered photons:

- Single-photon mode: The probability to scatter a photon is very low (0.001 for the existing TPOL), so that at most one photon is detected in the calorimeter).
- Few-photon mode: The probability is high enough that on average one photon per bunch crossing is observed. In the calorimeter a distribution ranging from one to a few photon is detected. The shape of the Compton spectra is still visible.
- Multi-photon mode: Per bunch crossing a large number of photons is scattered into the calorimeter (e.g. around 1000 for the LPOL).

2.1 A High Gain Fabry-Pérot Cavity

The new laser system will operate in the single- or few-photon mode. To have an averaged probability of 0.1 photon per interaction, the power of the laser system at the intersection with the lepton beam has to be around 5 kW, if a beam current of 1 mA and a crossing angle of 58 mrad are assumed. Such power levels cannot be reached with commercially available lasers. A Fabry-Pérot cavity located around the interaction point is therefore proposed [2] to boost the equivalent laser power to the required level. The expected gain of the device is 7.3×10^3, and the bandwidth is 7 kHz when pumped with an infrared laser of $\lambda = 1064$ nm.

The conceptual layout is shown schematically in Fig.2 and a detailed view is shown in Fig.3. The cavity surrounds the interaction point for a length of 2 m. The main part of the cavity is a tube made from stainless steel, with a wall thickness of around 0.3 cm. The tube is mounted on an optical table. The cavity mirrors, mounted on specially constructed mirror holders, are rigidly fixed to the table allowing the initial alignment of the mirrors. The cavity is thus a monolithic cavity. Tuning of the system is done by changing the frequency of the laser in a feedback loop, and not by varying the mechanical dimensions of the cavity. Such a design has been successfully employed at CEBAF [4].

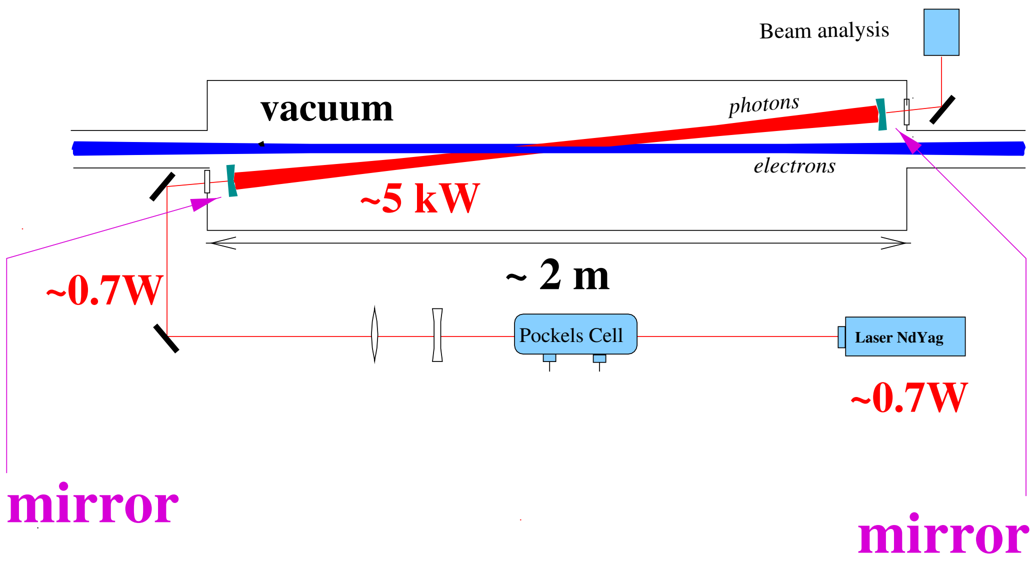

Figure 2: A schematic view of a Fabry-Pérot cavity and the laser system located around the electron beam. The power indicated in the cavity is the equivalent power a continuous wave laser must deliver to obtain the same Compton scattering rate.

The feedback system is able to correct for mechanical deformation of the cavity if they stay below $70\mu m$. Therefore it is essential that the cavity is stable at this level. The biggest problem is that of thermal expansion and contraction of the system, if the ambient temperature changes. A temperature change of $2°$C corresponds to the limit of an overall length change of 70 μm.

Temperature changes are coming from changes of the temperature in the tunnel, and from local heating effects of the beam pipe inside the cavity. The first problem can be solved by placing the whole system in a temperature controlled hut, maintaining a stable temperature

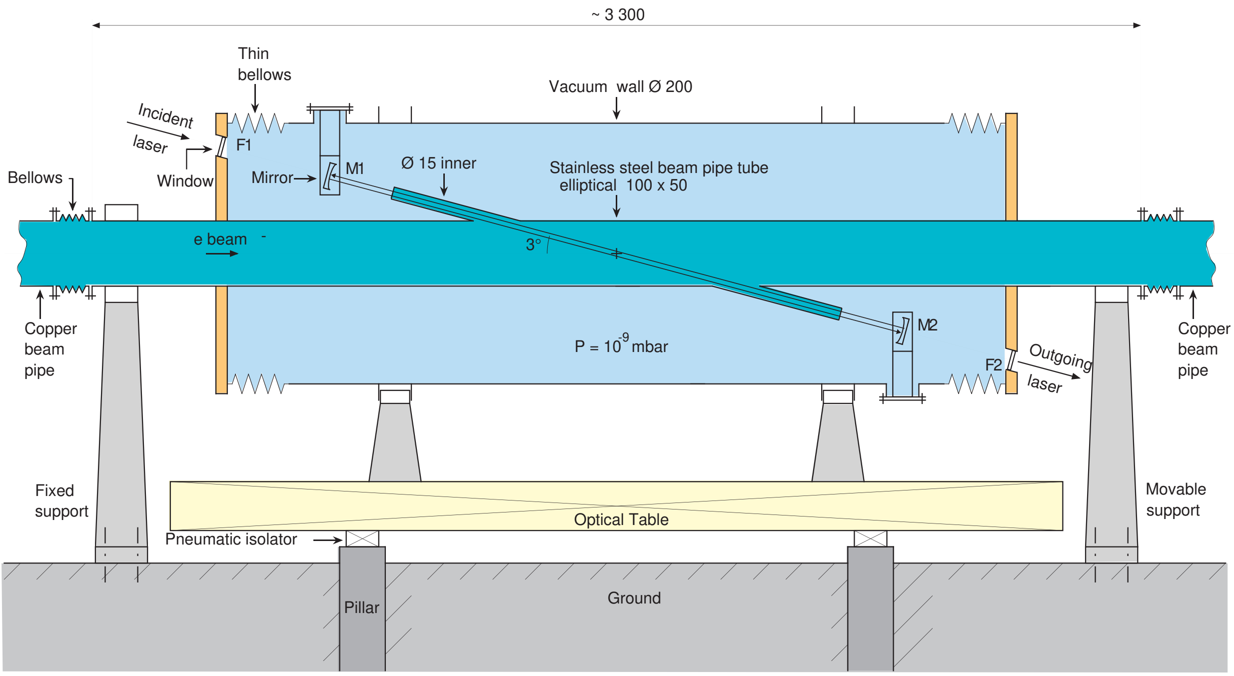

Figure 3: Layout of the cavity

within $1°$C in the hut. The temperature of the beam pipe at the present LPOL location has been measured [5] for different intensities of the e beam (between 0 and 48 mA), and during different times within a fill. The maximum temperature variation found is about $\sim 2.5°$C. In addition, some heat will be produced by higher order modes induced by the beam due to the holes in the beam pipe needed for the laser tube. The power lost has been estimated to be 18 W during injection, and less than one W during normal running [6]. This should not present a problem, since in the current design, without considering heat conduction, purely by radiative cooling the beam pipe heats by less than one degree for 25 W of heating power.

Another important source of concern is vibrations. One source originates from ground motion. A careful study of these has been made in the HERA tunnel [7]. Other sources of vibrations under investigation come from the machine itself, through cooling water circulation, magnet power supplies, etc.

The design shown in Fig.3 takes these effects into account. Indeed, the optical elements of the cavity are mechanically decoupled from the beam pipe and are supported from a stable optical platform. The latter is isolated from the HERA tunnel through pneumatic isolators. The central part of the cavity is connected to two end pieces by means of two bellows. Only the end pieces are in contact with the beam pipe. The central part of the cavity therefore is effectively thermally isolated from the rest of HERA. Heat produced in the beam pipe surrounding the cavity can only be transmitted by radiation, not by thermal heat conduction. In addition the bellows act as a vibration filter, blocking vibrations in the machine from reaching the mirrors. Preliminary calculations suggest that this system will be insensitive to the level of temperature changes and vibrations expected in the tunnel.

2.2 Other Optical Components

In addition to the Fabry-Pérot cavity, there are a few other optical components mounted on the same optical table, in particular the laser source (Nd:YAG, a small power solid state laser). The role of the these external optical elements is twofold: the laser beam has to be transported into the cavity, and the properties of the laser beam have to be measured and monitored. The laser beam has to be highly circularly polarized (better than 99.5%), and should be focused in the center of the cavity with a waist of ~ 0.6 mm.

A layout of the optical system is shown in Fig.4. The main parameters of the laser (spatial mode TEM00, linewidth < 5 kHZ, coarse (fine) frequency tuning range 30 GHz (30 MHz)) are well adapted to the system for both pumping the cavity and locking the system into resonance.

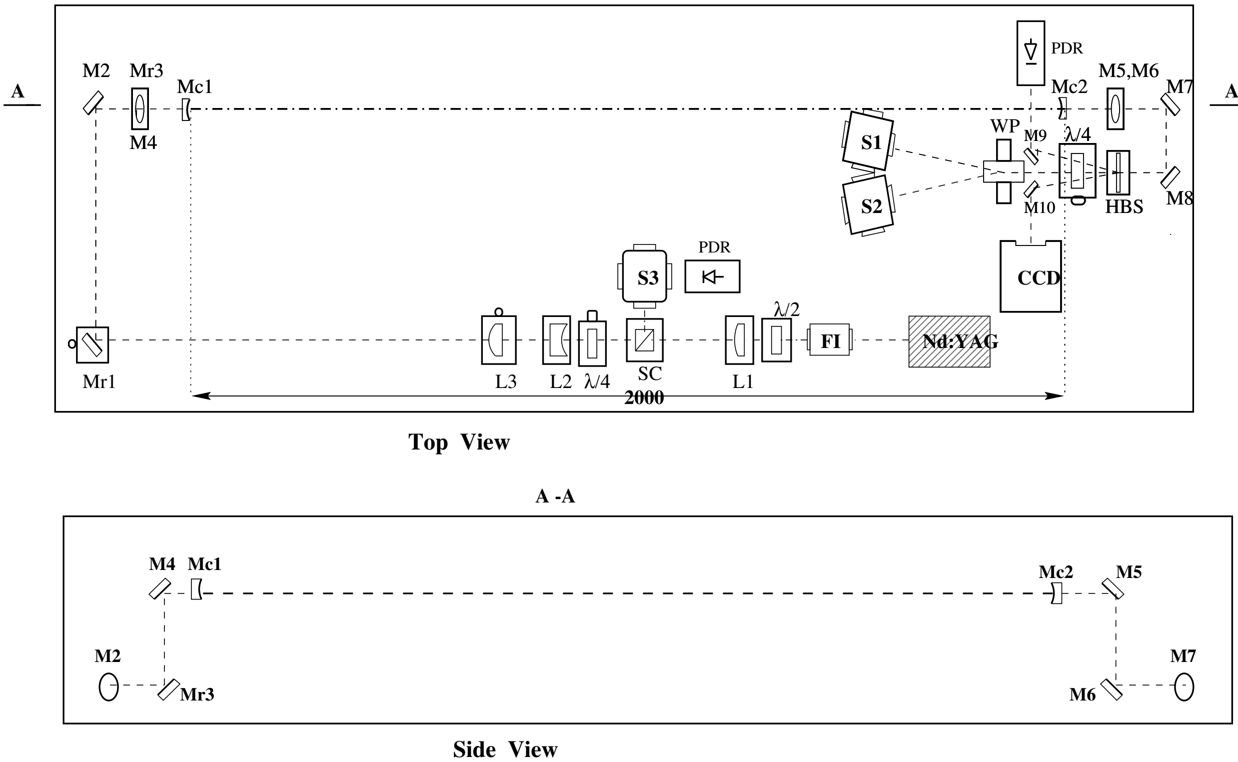

Figure 4: Layout of the optical components needed to operate the cavity, where FI is the Faraday insulator, Mc1 and Mc2 are two mirrors located inside the cavity, PDR, HBS, and WP stand respectively for photodetectors, holographic beam sampling, and Wollaston prism.

The laser is protected from light reflected from the entrance mirror through a Faraday insulator. A filter is used to linearly polarize the laser light. A system of $\lambda/2$ plate and beam splitter splits off a part of the beam and reflects it into an integrating sphere and photodetector. These are used to derive a signal for the mode-locking system.

A remote controlled $\lambda/4$ plate transforms the linearly polarized laser light into circularly polarized light. Switching between left and right polarized light is done by rotating the plate.

An optical telescope then focuses the laser beam into the cavity, and matches the focal point of the laser with that of the cavity. One of these lenses (L3 in the drawing) is remote-controllable, so that the focus can be fine-tuned during operation.

It is important that the mirrors used to reflect the light into the cavity do not disturb the circular polarization. Mirrors Mr1-Mr3 and Mr2-Mr4 are thus matched to have the same properties. In order to give the system enough degrees of freedom for matching the laser beam into the cavity, the mirrors Mr1 and Mr3 are furthermore remote-controllable.

A small fraction of the laser power exits the cavity and is reflected into a system of optical measurement devices. They are designed to determine the exact polarization of the laser light and to measure the power of the laser beam.

2.3 Radiation Effects on the Cavity Mirrors

A particular concern is the level of radiation exposure of the optical elements of the cavity, throughout its lifetime. During the month of July and August 2000, tests were done in HERA to investigate the effects of radiation on the proposed mirrors. The Laboratoire des materiaux avancés (IPN LYON) lent us two mirrors from the same batch used for the CEBAF cavity. These mirrors were installed next to the HERA beam pipe, at the same place where the final cavity will locate. One mirror was exposed directly to the radiation levels, the other one was shielded by 2 mm of lead. The dose absorbed by the mirrors was in both cases monitored with dosimeters, and was found to be ≈ 0.1 Gy/month inside the lead shielding, and around 10 times more without any shielding.

After the exposure both mirrors were tested and the quality of the mirror coating was determined. Within the measurement accuracy no change in the properties of the mirrors were detected.

2.4 Data Acquisition System

The significantly higher rates with which data are taken with the new LPOL make an addition to the existing DAQ necessary. It is intended to continue to use the existing slow controls and monitoring system, and only to add a fast DAQ system to record and analyze the data from the few-photon operation of the LPOL. In its basic option the new LPOL DAQ consists of two almost independent subsystems:

- a laser and cavity control system and its auxiliary electronics for laser alignment, feedback control, switching and monitoring of the cavity power and polarization. This system is similar as that developed for the CEBAF polarimeter;
- a VME based fast DAQ system for the few-photon mode LPOL, which is adapted from the upgraded TPOL DAQ.

For a transition period the slow control will be handled through the DAQ of the existing LPOL system. However, a new system specific to this device will have to be added when the new LPOL will eventually take over the existing one.

2.4.1 Fast LPOL DAQ

The fast part of the DAQ for the new LPOL in essence consists of custom-made fast ADC's and TDC's, which are read out by a dedicated Power-PC based Multifunction Computing Core (MFCC), while a second Power-PC takes care of the analysis and control of the data. The bandwidth of the ADC allows for the transfer of two data words per HERA bunch, which is enough for the new system (calorimeter total energy and pedestal). The readout and storage of the data however will have to be handled differently from the TPOL to allow for the larger rates.

2.4.2 Laser and Cavity Control

The laser control system is taken from the similar system developed for the CEBAF polarimeter. The system has two operation modes: manual and automatic. Under manual control the operator has direct control of the moving parts with corresponding data displays. Under automatic mode the following procedures are implemented:

- Laser feed back startup: The feedback electronics is started and the finding of the resonance is monitored.
- Laser beam alignment: 4 mirror motors, 8 monitoring diodes from 2 four cell quadrants, and beam transmission monitors are used to control the laser beam. A CCD camera permits a visual control of the resonant modes present in the cavity.
- Run control: Based on instructions received from the main run control, parameters like the light polarization, the power etc are varied and monitored.

All components in the system are commercial ones, except for the laser feedback electronics [1].

2.5 Calibration

One of the main advantages of operating the LPOL in the single-photon mode is the simplicity in the calibration of the detector. The energy spectra of the photons scattered into the detector have a simple physical meaning, and provide a number of unambiguous calibration points for the energy calibration of the detector. The main idea is to use the Compton edges for 1, 2, and maybe three photons, and the bremsstrahlung edge in the energy spectra, to define the energy scale of the calorimeter. In Fig.5 the spectrum (left) and the differential spectrum (right) for a simulated operation of the device with $n_\gamma = 0.1$ and $n_\gamma = 2$ is shown. Clearly visible are the locations of the single and double Compton peaks, and the position of the bremsstrahlung edge. Preliminary studies showed that this procedure allows a calibration of the device on a few per mill level.

To estimate the precision with which the polarization can be measured with this device, a number of systematic effects have been simulated and their impact on the polarization has been studied:

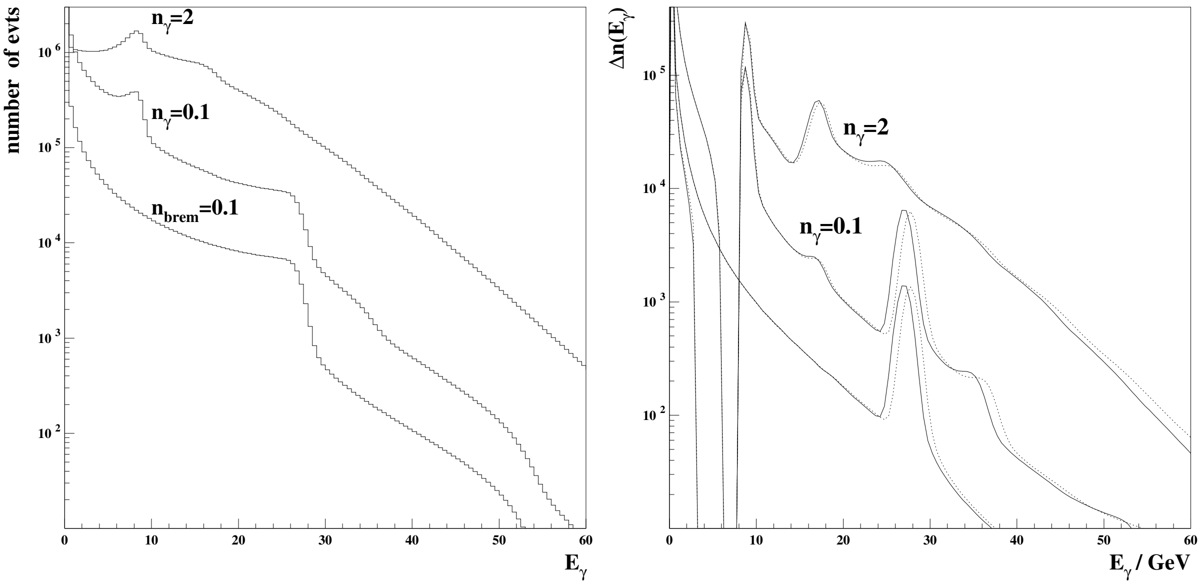

Figure 5: Compton spectra (left) including background, and differential spectra (right), for $n_\gamma = 0.1$ and 2. The dotted curves on the right are obtained by including a 1% nonlinear contribution in the energy calibration of the calorimeter. The lowest curve is an estimate of the background, obtained from the simulation when the laser is off.

- The knowledge of the energy scale of the calorimeter translates into an error on the polarization. Simulations have shown that a 0.5% uncertainty of the energy scale corresponds to an error of the polarization of 0.1% for a 50% polarization.

- If a nonlinear component exists in the response of the calorimeter this changes the analyzing power and therefore the measured polarization. However, a 1% effect at 10 GeV leads to a very large non-linearity in the position of the peaks (see right plot of Fig.5). Therefore, such a nonlinear effect can be controlled at the few per mill level. Assuming a possible residual non-linearity of 0.2% at 10 GeV we find a contribution to the uncertainty of the polarization of a few per mill.

- The polarization of the laser light inside the cavity is the same as the polarization of the light entering the cavity within 0.1%, as measured with the CEBAF cavity.

- Fluctuations of the laser power inside the cavity would change the form of the spectra, and in turn would influence the way in which calibration constants are derived from the spectra. From CEBAF such fluctuations are known to be controllable to better than 0.5%, which translates into an error of the polarization of 0.05%.

- The shape of the spectra is modified by additional material in front of the polarimeter. As an example in Fig.6 the effect of an additional 10% of a radiation length of material in front of the polarimeter is shown. At 50% beam polarization, this translates into an error of the polarization of around 0.3%. Therefore it is important that the amount of the material in front of the polarimeter is carefully controlled at the 1% of a radiation length level.

- The properties of the electron beam directly influence the distribution of photons on the front face of the calorimeter. With a well calibrated device, with a homogeneous response across the calorimeter, the influence of this can be reduced to the level of a few pre mill. In addition it is planned to install a fiber detector in front of the calorimeter. This detector will be able to measure the position of the Compton cone. Therefore corrections can be applied as a function of the Compton cone position. This scheme only works if enough data can be accumulated fast enough by the system, on a time scale which is small compared to the typical time scale of a precise determination of the polarization in the machine. This is clearly the case when a precise determination of the polarization is done within a few minutes, so it should not present any problem to the new system under construction.

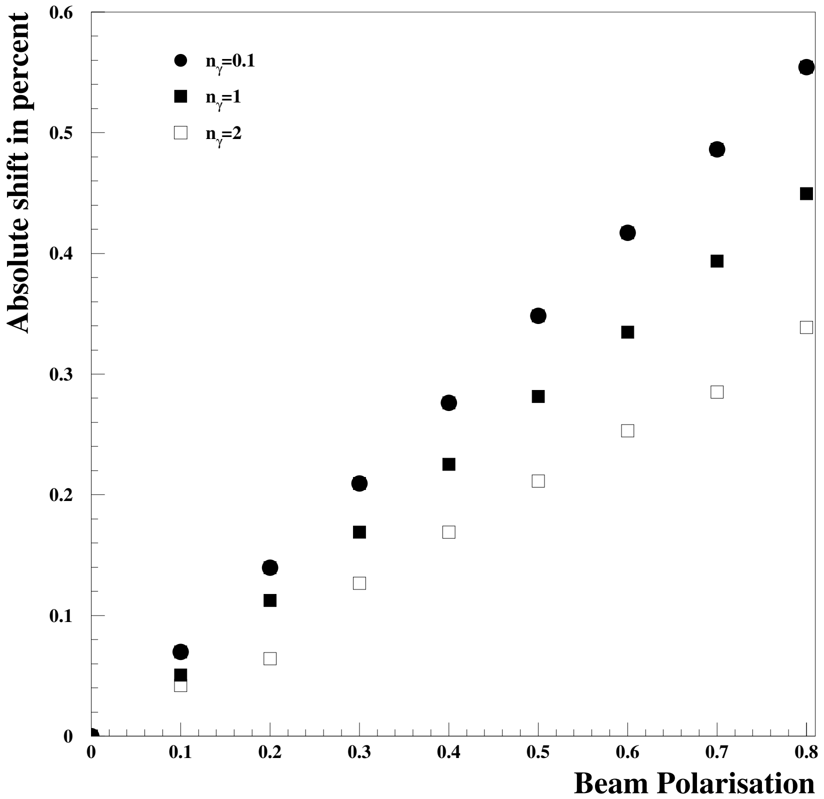

Figure 6: Change in the polarization, if the photon beam has to traverse an additional 10% of a radiation length of material in front of the calorimeter, for different levels of beam polarization and for different Compton photon rates.

In conclusion, it seems likely that the systematic errors of the polarization can be controlled very well with the new LPOL. An essential condition is that the LPOL can be operated in the single-/few-photon mode, and that the polarization is precisely determined within a few minutes, on a time scale short in comparison to the intrinsic variations of the polarization in the machine.

3 The Necessities of Having a Fast and Precise Polarization Measurement

Physics with polarized lepton beams will be a central part of the physics program of HERA after the luminosity upgrade. The basic program has been described in a series of workshops [8], [9] and [10]. We will discuss first in Sec.3.1 the role the polarization will play in this and in Sec.3.2 its roles from the machine's point of view.

3.1 The Physics Case

Three topics are of particular relevance: the charged current (CC) cross-section measurement, the right-handed CC and the measurement of the light quark electroweak couplings. In the following each of these topics will be discussed in detail.

3.1.1 Charged Current Cross-Section Measurements

A precise determination of CC cross-section at HERA can serve as a sensitive test ground of the Standard Model. One test is the helicity structure of the CC. Another such test is the precise measurement of the total cross-section, and its interpretation in the Standard Model.

One particular interesting quantity is the mass of the W boson. Although no large data sample of directly reconstructed W bosons is available at HERA, a precise indirect determination of the W mass is possible. As an example, with $1000\,\mathrm{pb}^{-1}$ CC and NC data and a polarization of 70$\%$, a total systematic error of 1% leads to a determination of M_W with an accuracy of 55 MeV. This determination would be competitive to the LEP and Tevatron results and, because the W is accessed via the t channel at HERA, it would provide a test of the universality of the Standard Model.

3.1.2 Search for Right Handed Charged Currents

In the Standard Model of the electroweak and strong interactions, CCs are carried by left-handed W bosons. Right-handed CCs should not exist. So far no experimental evidence for right-handed CCs has been found. The present limit, expressed in terms of the mass of a right-handed W boson, is 750 GeV at 95% confidence level (CL) [11]. In studying collisions between polarized leptons and unpolarized protons, as will be the case at HERA after the upgrade, sensitive and direct searches for right-handed CCs can be done.

To estimate the reach of HERA we shall assume the following parameter: HERA operates with two helicities of the lepton (electron or positron) beam. The level of polarization for each helicity state is taken to be 50%. For each helicity an integrated luminosity of $250\,\mathrm{pb}^{-1}$ is considered. This corresponds to about one year running per helicity state at the nominal luminosity of the machine after the upgrade.

The observed CC cross-sections as a function of the lepton polarization P is given by

$$\sigma^{e^-}_{\mathrm{obs,CC}}(P) = \frac{1-P}{2}\sigma^{e^-}_L + \frac{1+P}{2}\sigma^{e^-}_R \tag{1}$$

where $\sigma^{e^-}_R$ is the right-handed CC cross-section, $\sigma^{e^-}_L$ the left-handed CC cross-section, and P is the luminosity weighted polarization valid for the whole data sample:

$$P = \frac{\sum_i^{N_{\mathrm{run}}} \int_{t_{\mathrm{min},i}}^{t_{\mathrm{max},i}} P_i(t)\mathcal{L}_i(t)dt}{\sum_i^{N_{\mathrm{run}}} \int_{t_{\mathrm{min},i}}^{t_{\mathrm{max},i}} \mathcal{L}_i(t)dt} \; . \tag{2}$$

In this equation the number of runs taken is denoted with N_{run}, and $(t_{\mathrm{max},i} - t_{\mathrm{min},i})$ is the duration of the i-th run, $\mathcal{L}_i(t)$ and $P_i(t)$ are the instantaneous luminosity and polarization respectively.

Using Eq.(1) a measurement can be performed of the right-handed CC cross-section, if the two data samples taken with positive and negative helicities are combined. Such a measurement with an assumed data sample of 250 pb^{-1} is shown in Fig.7 for data at large $Q^2 > 1000\,\mathrm{GeV}^2$.

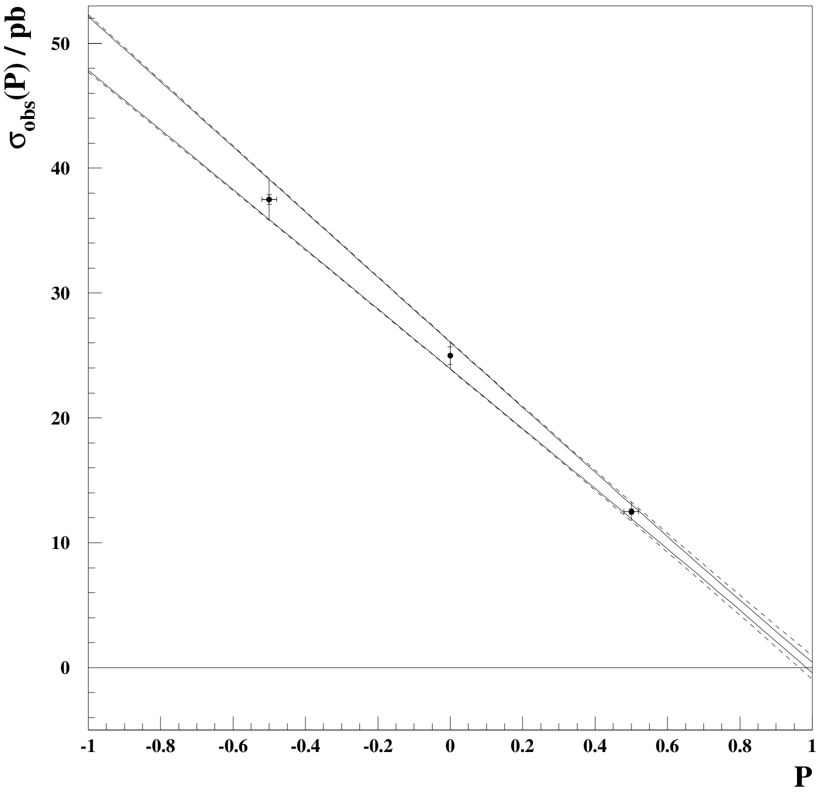

Figure 7: Measured charged current cross-sections at positive and negative helicities, for $Q^2 > 1000$ GeV, and extrapolation to the point of $P = +100\%$. The hashed band indicates the extrapolation error assuming a data sample of 250 pb^{-1} per point (see text for more details).

To estimate the uncertainty of the right-handed CC cross-section, it is convenient to define the ratio $r = \sigma^{e^-}_R / \sigma^{e^-}_L$. This ratio should be zero in the Standard Model. From the observed CC cross-sections, $\sigma_{\mathrm{obs,CC}}$, at $+|P|$ and at $-|P|$, the ratio of the measured quantities $R =$

$\sigma^{e^-}_{\mathrm{obs,CC}}(|P|)/\sigma^{e^-}_{\mathrm{obs,CC}}(-|P|)$ is defined, which can be expressed as a function of the theoretical ratio of cross-sections, r, as

$$R(|P|) = \frac{\alpha + r}{1 + \alpha r}\ , \ \text{with} \quad \alpha = \frac{1 - |P|}{1 + |P|}\ . \tag{3}$$

From this one obtains:

$$r = \frac{R - \alpha}{1 - \alpha R}\ . \tag{4}$$

Fig.8 shows how $(\delta r)_{\mathrm{stat}}$ changes with the uncertainty on the polarization measurement $(\delta P)_{\mathrm{stat}}$. The two solid curves shown correspond to different levels of polarization of the lepton beam, of

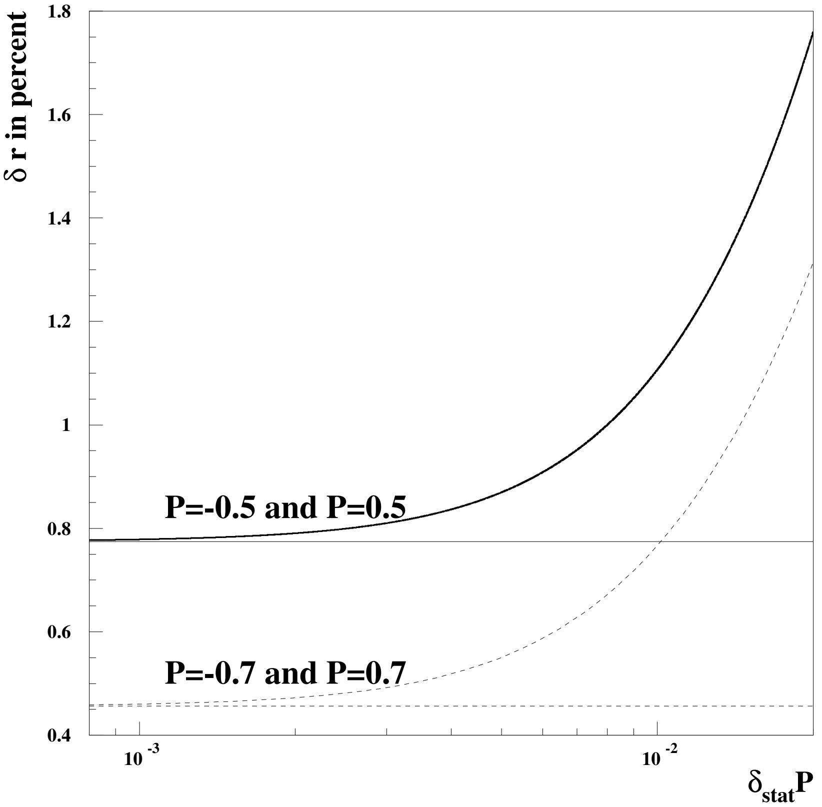

Figure 8: Relative uncertainty of the right-handed charged current cross-section, as a function of the error of the polarization measurement. The solid curve is for 50% polarization, the dashed one for 70% polarization. Also indicated is the contribution to the uncertainty which does not depend on the polarization.

50% and 70%. It is clearly visible that a higher polarization minimizes the error on r.

In this measurement, one must carefully distinguish systematic uncertainties which are proportional to the CC cross-section (scaling systematics: luminosity uncertainty, hadronic energy scale uncertainty, etc) from those which are independent of the cross-section (additive systematics: background). A measurement of the right-handed CC cross-section is only sensitive to the second part, the additive systematic uncertainties. The luminosity uncertainty, at least in first order, does not enter the extrapolation to $P = +1$. From the current CC analysis in the

H1 experiment for the high Q^2 analysis ($Q^2 > 1000\,\mathrm{GeV}^2$), the first type of uncertainties is estimated to be around 4%. Therefore, to a good approximation, the right-handed cross-section uncertainty depends only on the statistical accuracy of the cross-section measurements and on the statistical and systematic uncertainties of the polarization measurement.

From these studies, one concludes that in order that the errors from the polarization do not limit the final accuracy of the measurement, the total error of the polarization should be kept around 2×10^{-3}.

This simple picture changes slightly if the polarization measurement introduces correlation between the measured cross-section. If e.g. systematic uncertainties are fully correlated between the cross-sections at different beam helicities, it can be easily shown, that

$$(\delta r)_{\mathrm{sys}} \approx \frac{(\delta P)_{\mathrm{sys}}}{2}\,, \tag{5}$$

where $(\delta P)_{\mathrm{sys}}$ is the correlated part (scaling or additive) of the systematic uncertainty of the polarization measurement. Such effects therefore should be controlled at the 0.5% level in order not to limit the precision on the final result.

The reach of HERA compared to other experiments is best expressed in terms of a mass of a hypothetical right-handed W boson. Given the current estimates of systematics, and assuming a high precision determination of the polarization to 0.2%, the results are summarized in Fig.9. It shows clearly that for competing with the Tevatron we need a very large data sample. If the uncertainties can be tightly controlled, the reach of HERA becomes comparable to that of the Tevatron with the advantage of a pure and direct measurement.

In conclusion the investigation of the right-handed CC requires the highest possible precision from all parts of the experiment and the machine: luminosity, polarization and detector systematics all should be controlled very tightly to maximize the reach of HERA.

3.1.3 Neutral Current Cross-Section Measurements

The cross-section for the neutral current (NC) events in polarized lepton-proton scattering can be written as :

$$\begin{aligned} \sigma_{\mathrm{NC}}^{e^\pm p} &= \frac{2\pi\alpha^2}{xQ^4}\left(H_0^\pm + PH_P^\pm\right) \quad \text{with} \\ H_{0,P}^\pm &= \left(1+(1-y)^2\right)\, F_2^{0,P} \;\mp\; \left(1-(1-y)^2\right)\, xF_3^{0,P}\,. \end{aligned} \tag{6}$$

For large Q^2, where the longitudinal function F_L can be neglected, $F_2^{0,\mathcal{P}}$ and $xF_3^{0,\mathcal{P}}$ are the deep-inelastic-scattering structure functions and contain linear combination of the quark densities and quadratic functions of the vector and axial couplings of the fermions to the Z^0. By measuring the NC cross-section for different lepton charges and different helicity states the vector and axial coupling constants v_u, v_d, a_u and a_d can be measured.

The analysis consists of a χ^2 fit to four NC differential cross-section measurements: $e^-_{+|P|}$, $e^-_{-|P|}$, $e^+_{+|P|}$ and $e^+_{-|P|}$. Unknown parameters of this fit are the light quark electroweak couplings a_u, v_u, a_d and v_d.

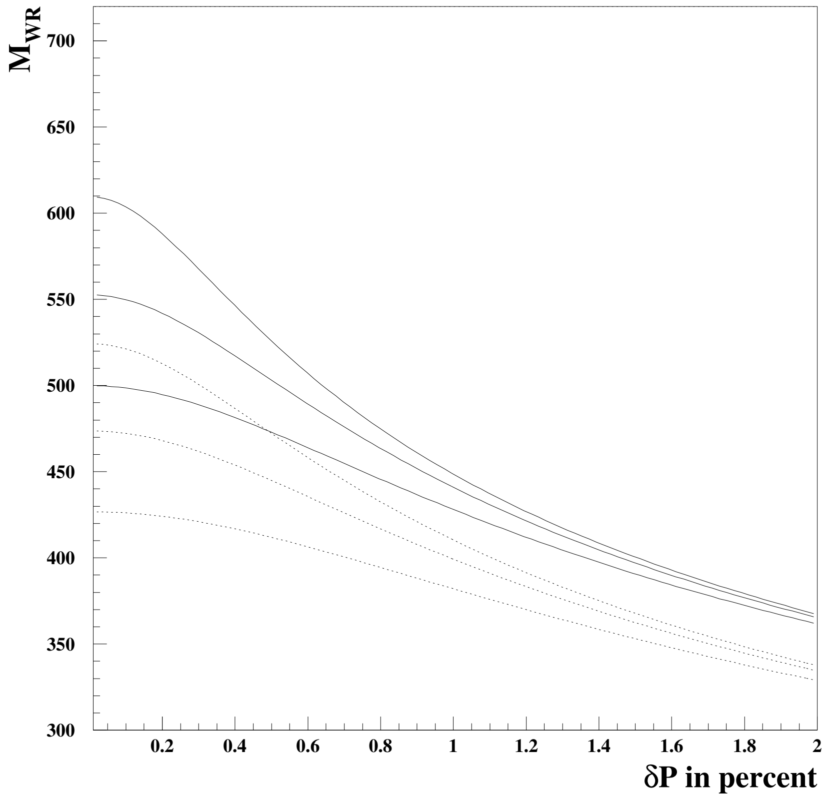

Figure 9: Possible exclusion limit (95% CL) obtainable at HERA, for a right-handed W boson, as a function of the precision of the polarization measurement. Full curves are for $P = 0.7$, dotted ones for $P = 0.5$. For each polarization value, the top curve corresponds to $1000\,\mathrm{pb}^{-1}$, the middle one to $500\,\mathrm{pb}^{-1}$, and the lower one to $250\,\mathrm{pb}^{-1}$.

In Fig.10 the 1σ contour plot in the $a_u - v_u$ plane is shown. It was assumed that at each of the four data points an integrated luminosity of $250\,\mathrm{pb}^{-1}$ is available. The ellipse corresponds to a 50% lepton beam polarization. Also shown is a second shifted ellipse which corresponds to the result of a measurement if a systematic shift of 1% is present in the polarization measurement. From this curve it is clear that such systematic effects on the polarization should be controlled to be better than one percent.

In conclusion the determination of the NC coupling constants for light quarks at HERA will provide a stringent test of the consistency of the Standard Model. To achieve a precision comparable to that of LEP a determination of both luminosity and polarization to around 1% is needed.

3.2 Other Considerations

In this section, we discuss a number of other considerations which also point to the necessity of having a fast and precise polarization measurement.

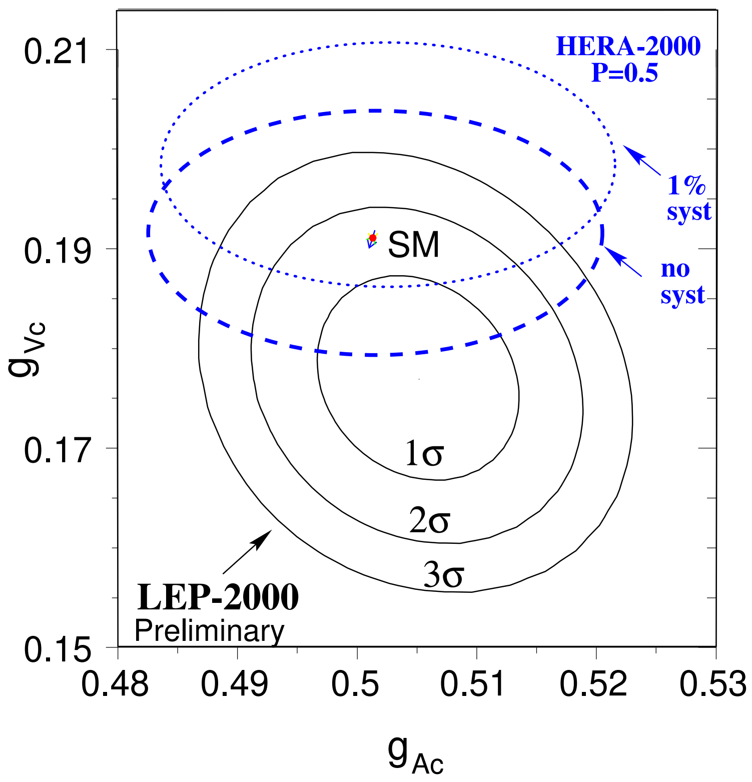

Figure 10: Couplings constants for up-type quarks, as measured at LEP, and expected measurement at HERA.

3.2.1 Luminosity - Polarization Correlations

The effective polarization needed for the different measurements discussed is a luminosity weighted sum, as defined in Eq.(2). Based on typical HERA run durations of around 12h, and a typical turn-on time of the experiments after the declaration of physics, the effective polarization in the machine is reduced from its asymptotic value by $6-10\%$ (e.g., assuming an asymptotic polarization of 50%, averaged over the run the luminosity weighted polarization is may be 47%).

In Fig.11, the measured polarization from a typical HERA fill is shown, as a function of the bunch number. Two things are visible: there are clear differences between colliding and non-colliding bunches, and there appears to be a clear structure in the polarization of the colliding bunches. In Fig.12, the variation of the polarization is shown as a function of time throughout a fill. The observed variations are seen by both polarimeters. Typical time-scales for these variations are a few 10 minutes. Taking both plots together it is important that the polarization of individual bunch can be tracked with sufficient accuracy ($< 1\%$) on a time-scale of a few minutes per point. In this way, a correction to the overall polarization can be done, based on the actual polarization of the bunches and on their individual behavior.

Since the luminosity is highest early in the fill, it would be good that these data are also used in the analysis. For this, one has to take possible correlations between the polarization and the luminosity into account. There are two possible sources of correlation: bunch-to-bunch

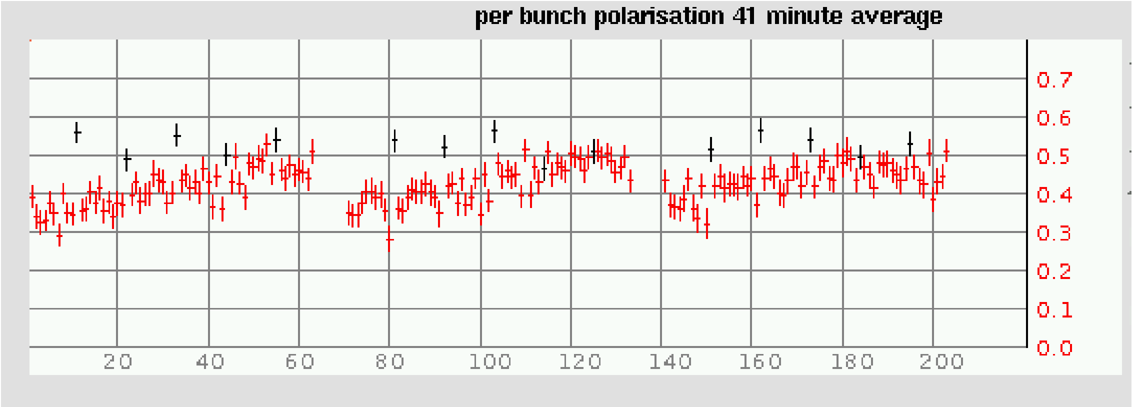

Figure 11: Transverse polarization measured during the test of the new TPOL DAQ system, as a function of the bunch number. Data points with polarization $P \approx 0.55$ are the non-colliding bunches.

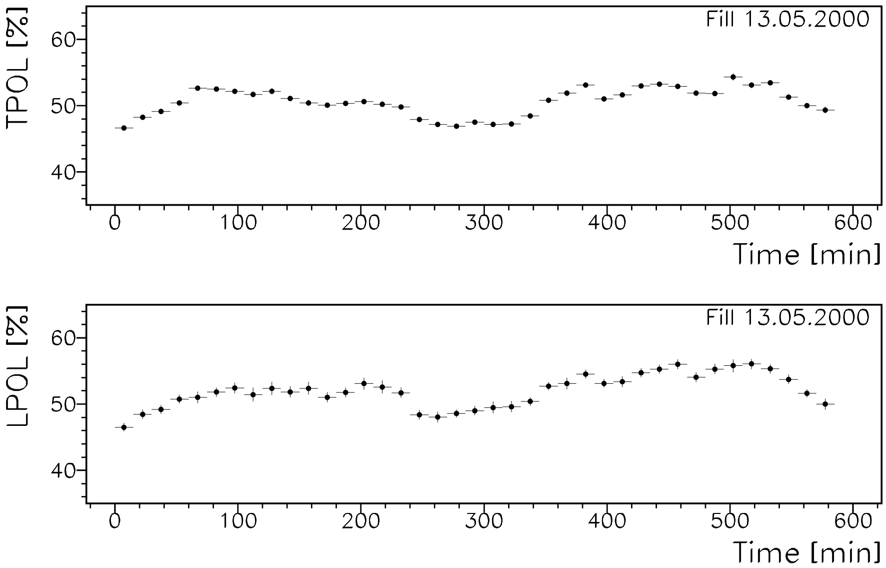

Figure 12: Transverse and longitudinal polarizations averaged over all bunches, for a given fill, as a function of time. Time variations are observed simultaneously by both calorimeters.

correlation and time evolution. The latter source has already been described above. To control it one must measure accurately the polarization during the early phase of the polarization during its buildup. This implies a very fast polarimeter.

The time evolution of the bunch-to-bunch correlation coefficient between P and a variable X is defined as:

$$C^t(P,X) = \frac{\left[\sum_{i=1}^{N}(P_i - \overline{P})\right]\left[\sum_{i=1}^{N}(X_i - \overline{X})\right]}{\sqrt{\sigma_P^2 + \sigma_X^2}} \tag{7}$$

with $\overline{P}$ and $\overline{X}$ being respectively the average of P_i and X_i. The summation is over all colliding bunches N, and X can be e.g. the luminosity $\mathcal{L}$, the lepton beam intensity I_e or the proton beam intensity I_P. In Fig.13(a) the polarization as a function of time is shown for a typical HERA fill. For this fill, the correlations to luminosity, the electron and proton currents are shown in Fig.13(b), (c), and (d). The luminosity and the current intensity data are taken every 10 s and the polarization is calculated for 10 min intervals.

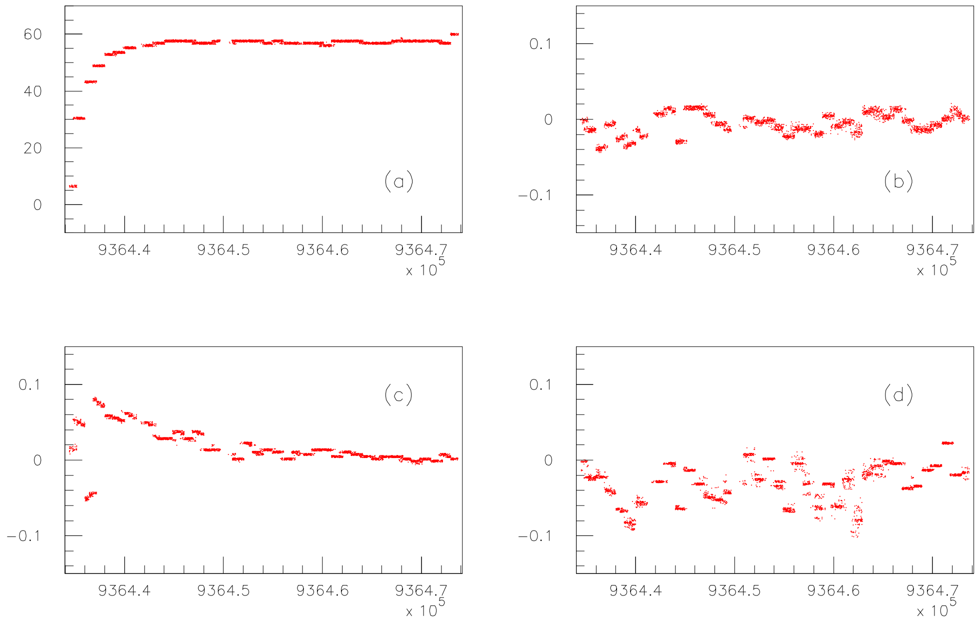

Figure 13: Polarization (a) and its correlation with luminosity $C^t(P, L)$ (b), lepton beam intensity $C^t(P, I_e)$, and proton beam intensity $C^t(P, I_P)$ (d) as a function of time for one typical fill.

With the present accuracy it is, however, difficult to determine if a significant level of correlation exists. To do so a precise bunch-by-bunch polarization measurement is desirable.

3.2.2 Optimization of the Polarization

From the above discussions it is clear that the most important input to the physics reach of HERA for polarized physics is, aside from the luminosity, the degree of polarization in the machine. The higher the polarization, the smaller the errors are. The optimization of the polarization therefore will play a crucial role in the running of the machine after the upgrade.

One way to reach higher polarization is to take advantage of the time-to-time and bunch-to-bunch fluctuations (see Figs.11 and 12). To use this possibility, a fast polarimeter, allowing a precise bunch-by-bunch polarization measurement, is required.

At the moment the polarization is optimized in an empirical procedure, by using so-called harmonic bumps. These are ensembles of magnets, arranged at different locations symmetrically around the ring. They are used to spin-match the machine, and also to compensate for the effect from magnet misalignments.

An important input in the procedure is the effect on the polarization. A fast and precise measurement of the polarization can help to speed up the procedure, to detect changes in the polarization faster, and to start corrective actions earlier before a significant loss of polarization occurs. The result of an adjustment of the harmonic bumps is shown in Fig.14. The steps observed in the polarization are the result of an optimization. As can be seen the time between adjustments is of the order of hours, before the full effect of an optimization can be judged.

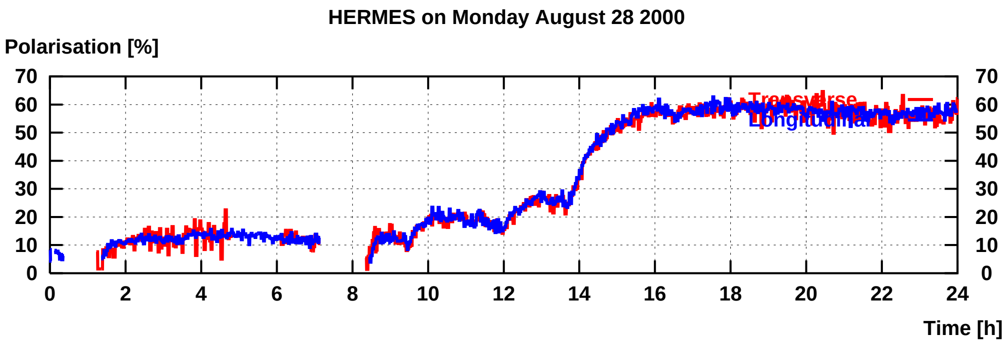

Figure 14: Development of the polarization throughout a typical HERA fill. Visible are a number of increases of the polarization, which are the result of harmonic bump optimizations.

A fast and precise measurement of the polarization can help in two ways:

- a change of the polarization after a change in the machine parameters can be quickly detected. A feedback therefore is available to the machine on whether or not a particular operation was successful;
- if the measurements is precise enough a determination of the speed with which the polarization changes after an operation can be made. This information can be used to determine the theoretically possible maximum polarization in the machine, if no further changes are done. Thus at least in theory it is possible to perform a number of optimization steps within a relatively short time, optimizing the asymtotic polarization without having to wait each time for the full effect of the preceding optimization step.

Note that in order to avoid oscillations the measurement does not only need to be fast, but also precise, to avoid taking decisions based on statistical fluctuations.

To estimate what one could gain with a fast and precise polarization measurement, a simple model is considered. The rise-up curve is modeled by

$$P(t) = P_\infty - (P_\infty - P_0)e^{-\frac{t-t_0}{\tau}} \tag{8}$$

where P_0 is the polarization at $t = t_0$ and $P_\infty = P_{\mathrm{ST}}/\tau_{\mathrm{ST}} \times \tau$ with $P_{\mathrm{ST}} = 0.916$, $\tau = 43.2$ s. τ_{ST} is the intrinsic rise-time of the polarization in the machine, and τ the time of the measurement.

It is conceivable to install a simple feedback in the machine, which would help keeping the polarization at a maximum. This procedure would rely on a fast and precise determination of the polarization in the following ways: over a time interval ΔT the polarization is measured each a number of times, e.g. every 6 s, and the data points are fitted with a simple model, as e.g. given in Eq.(8). If the fit is based on data point of sufficient precision, a prediction can be made whether the polarization in the machine is stable, or is changing in a significant fashion. Among a large number of decision criteria, we have investigated the determination of the asymtotic value P_∞: after a period ΔT one decides if a significant polarization change is observed if the uncertainty δP_∞, determined by the fit, is smaller than a given value. However, such criteria are reliable only for a short period of time because of machine changes and would be, in this case, more efficient if applied on the non-colliding bunches polarization measurement.

Fig.15 shows ΔT as a function of P_0 (see Eq.(8)) for $P_\infty = 0.5$ and a required $\delta P_\infty = 1\%$. The three curves correspond to different polarization measurement accuracies $\delta P = 0.1\%$ (colliding bunches), 0.3% (non-colliding bunches) and 1% (individual bunch).

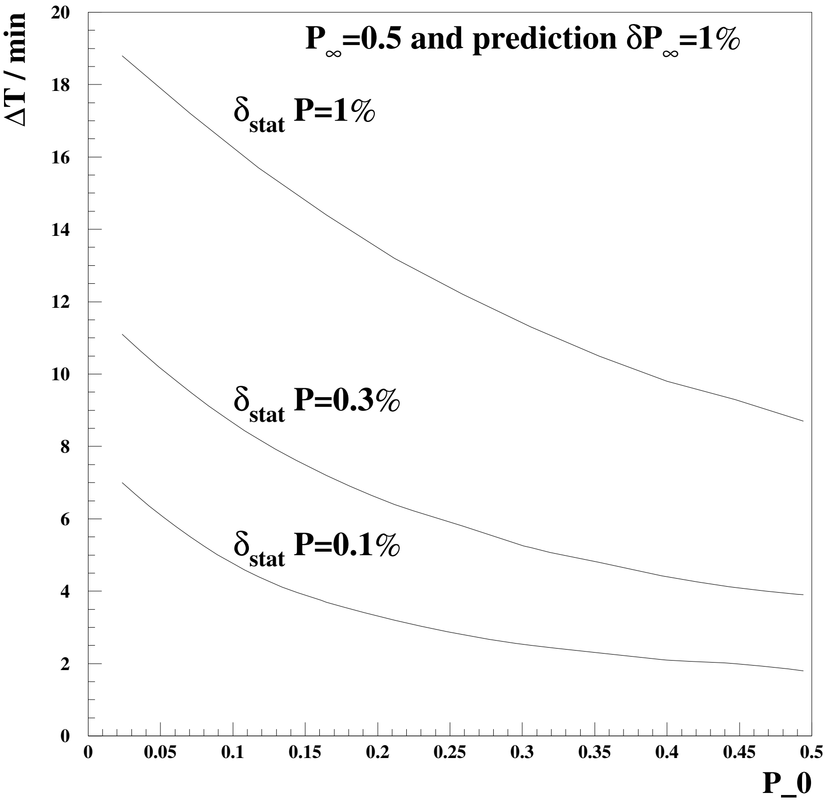

Figure 15: ΔT as a function of P_0 (see text) for $P_\infty = 0.5$ and $\delta P = 1\%$. The three curves correspond to different polarization measurement accuracies $\delta P = 0.1\%$, 0.3% and 1%.

From this simple simulations and from comparisons to typical HERA fills, it is found that reliable statements can be made if the polarization is measured over periods of a few minutes with an accuracy of a few per mill over a few seconds.

4 Conclusion

The new longitudinal polarimeter under construction uses a Fabry-Pérot cavity to significantly gain the effective power of a laser light. The increased power will enable us to operate the LPOL in the single-/few-photon mode, and still reaching a high statistical accuracy of 0.2%. The new polarimeter has a number of important advantages over the existing ones:

- The polarimeter can be calibrated using the same data as for the polarization measurement;
- Systematic errors can be tracked and controlled based on information obtained from the data;
- Fast and reliable feedback can be given to the machine, helping to optimize the polarization.

The precision which this device should be able to reach will be around $0.2 - 0.4\%$ on the polarization. This will guarantee that the physics potential of HERA is not limited by the polarimetry, and that high precision measurements for the study of neutral and charged currents are possible.

Based on all investigations made so far, we are confident that the new polarimeter will meet the goals both in terms of performance and in terms of reliability.

References

[1] E. Barrelet *et al.*, "Letter of Intent to Upgrade the Longitudinal Polarimeter", DESY PRC 00-02, April, 2000.

[2] E. Barrelet *et al.*, "Proposal to Upgrade the Longitudinal Polarimeter", DESY PRC 00-02, Oct., 2000.

[3] A. A. Sokolov and I. M. Ternov, *Sov. Phys. Doklady* **8** (1994) 1203.

[4] See http://www.cebaf.gov/compton for a complete documentation.

[5] P. Schuler, private communication.

[6] S. Wipf, private communication.

[7] DESY report.

[8] Proceedings of the 1987 HERA Physics Workshop, ed. R.D. Peccei (DESY, Hamburg, 1988).

[9] Proceedings of the 1991 HERA Physics Workshop, ed. W. Buchmuller and G. Ingelman (DESY, Hamburg, 1992).

[10] Proceedings of the 1995/1996 Future Physics at HERA Workshop, ed. G. Ingelman, A. De Roeck and R. Klanner (DESY, Hamburg, 1992).

[11] D0 Collaboration, *Phys. Rev. Lett.* **76** (1996) 3271.